




Enhancing impedance control in microstrip lines using the Taguchi approach

Mohd H.S. Alrashdan¹ · Zouhair Al-qudah² · Mohammad Al Bataineh^{3,4} 

Received: 19 May 2025 / Accepted: 20 August 2025
© The Author(s) 2025

Abstract

Microstrip Transmission Lines (MTL) are crucial components in various electronic and communication systems because of their streamlined design, affordability, and wide frequency range. However, achieving precise control over their characteristic impedance (CI) is essential for optimal performance. This article utilises the Taguchi method (TM) to optimise the CI of MTL by systematically evaluating seven input control factors: strip width, strip thickness, dielectric height, ground plane thickness, frequency, dielectric conductivity, and conductor conductivity. Each factor is assessed at three different levels to find the best conditions for impedance regulation. Our findings reveal that strip width and dielectric height significantly influence the CI. Validation through analysis of variance (ANOVA) confirms the effectiveness of the TM. To demonstrate versatility across different application requirements, this work targets multiple CI of MTL values of (55 Ω and 70 Ω). As a practical application, MTL with a CI of 70 Ω were developed and analyzed through simulations in COMSOL Multiphysics, achieving a capacitance of 6.3829×10^{-11} F/m, resistance of 213.22 Ω /m, propagation constant of $(1.5230 + 505.33i)$ m⁻¹, shunt conductance of 2.5687×10^{-17} S/m, inductance of 3.1276×10^{-7} H/m, and CI of $(70.000 - 0.21097i)$ Ω . This study provides a systematic approach for designing MTL customised for specific uses, removing the reliance on extensive trial-and-error approaches.

Keywords Microstrip transmission lines · Taguchi method · Characteristic impedance · COMSOL simulation · ANOVA · MESA

1 Introduction

Microstrip Transmission Lines (MTL) are an integral part of modern communication systems (Fertas et al. 2015), essential for ensuring the efficient transmission of electromagnetic

signals in a wide range of electronic devices. This innovative transmission line configuration has gained widespread popularity due to its unique structure (Wu et al. 2021) and versatile applications across a spectrum of electronic systems (Mitra et al. 2019).

The significance of Microstrip Transmission Lines (MTL) lies in their capability to provide a compact and lightweight solution for high-frequency signal transmission (Han et al. 2022). These lines are widely employed in microwave and RF (radio frequency) circuits (Pinheiro and Rehder 2018), making them fundamental components in communication systems (Rana and Rahman 2022), radar systems (Nagy 2022), satellite communication (Basit et al. 2020), wireless networks (Colaco and Lohani 2020), aerospace (Nicholson et al. 2016), medical equipment (Iqbal et al. 2019), and consumer electronics (Le et al. 2019). They are commonly used in the design of antennas, filters, couplers, and impedance-matching networks (Joseph et al. 2021; Couraud et al. 2021).

The adaptability of MTL makes them suitable for diverse applications, ranging from high-frequency microwave circuits to complex integrated systems. Despite their widespread

✉ Mohammad Al Bataineh
mffbataineh@uaeu.ac.ae
Mohd H.S. Alrashdan
moh.alrashdan@ahu.edu.jo
Zouhair Al-qudah
qudahz@ahu.edu.jo

¹ Department of Electrical Engineering, Al-Hussein Bin Talal University, Ma'an 71111, Jordan
² Department of Communication Engineering, Al-Hussein Bin Talal University, Ma'an, Jordan
³ Electrical and Communication Engineering Department, United Arab Emirates University, Al Ain, United Arab Emirates
⁴ Telecommunications Engineering Department, Yarmouk University, Irbid 21163, Jordan

use, MTLs have certain limitations, including the potential for signal losses—particularly at higher frequencies—due to factors such as radiation and dielectric losses (Chen et al. 2019). Impedance discontinuities caused by changes in line width, substrate properties, or component connections (Jin et al. 2022) can lead to signal reflections and mismatched impedances. Substrate tolerance and variability, manufacturing tolerances, and material variability can result in deviations from the intended characteristic impedance (CI), affecting the overall performance of the transmission line (Gazizov et al. 2019).

Researchers encounter several challenges in the design and implementation of MTL. These challenges include: (i) achieving precise impedance matching (Khaleghi et al. 2019; Li et al. 2022), (ii) minimizing signal losses (Zhang et al. 2021), and (iii) controlling radiation patterns (Abdulhameed et al. 2019)—all of which are critical to performance. Ensuring accurate impedance matching is essential to reduce signal reflection and enhance power transfer. Designers also face difficulties in maintaining consistent impedance, particularly when integrating MTLs with other circuit components. These challenges are exacerbated in high-frequency applications, where minor mismatches can lead to significant performance degradation. Moreover, substrate selection and fabrication tolerances add further complexity. As operating frequencies continue to rise, researchers must push the boundaries of existing designs and adopt more precise, robust design methodologies.

In high-frequency applications such as radar systems, satellite communications, aerospace electronics, and medical imaging devices, accurate impedance matching in MTLs is vital for minimizing reflection, maximizing power transfer, and preserving signal integrity. Even slight mismatches in characteristic impedance can cause substantial signal loss, electromagnetic interference, and degraded system performance. For instance, in radar front-end modules or implantable medical devices—where design constraints are stringent—the ability to design MTLs with predictable impedance characteristics can significantly reduce reliance on costly prototyping and iterative testing. Therefore, adopting a robust and systematic approach to impedance control is not only academically valuable but also critical to industrial applications.

Researchers and engineers employ various methods to achieve precise impedance matching in MTL, including: (i) MTL design and width adjustment (Cogollos et al. 2018), (ii) substrate selection with specific dielectric constant (ϵ_r) (Chung et al. 2021), (iii) adjusting the tapered widths (José 2022), (iv) stub matching using open- or short-circuited stubs (Gupta et al. 2023), (v) using balun transformers (Maktoomi et al. 2020; Fereshtian and Ghalibafan 2020), (vi) adding lumped elements such as inductors and capacitors (Kareem et al. 2023), and (vii) feedback

and tuning, where researchers use measurement tools like network analyzers to characterize actual performance and fine-tune the MTL for precise impedance matching (Al-Sawalmeh et al. 2022). These methods have primarily relied on trial-and-error approaches. This conventional technique entails making impromptu and intuitive modifications to the parameters of MTL, often necessitating extensive effort to attain desired results. Genetic Algorithms (GA) (Thajjiam 2025) have been applied to optimise single parameters of MTLs such as line width or substrate thickness. also Particle Swarm Optimization (PSO) (Ghewari and Patil 2025) has shown promise in dual-parameter scenarios. Neural network approaches have demonstrated capability in predicting impedance values but require extensive training datasets and lack transparency in the optimisation process (Prabhakar et al. 2024). Response surface methodology (RSM) has been used for three-parameter optimisation, but becomes computationally intensive for higher-dimensional problems (Xu et al. 2025). Unfortunately, this method focuses on optimising 2–3 parameters simultaneously, neglecting the complex interactions among all relevant design variables, it can consume significant time, lacks a systematic framework, and can lead to inefficiencies, increased costs, and inconsistent outcomes (Taguchi 1995). Additionally, it frequently neglects a thorough analysis of robustness, making it difficult to ensure consistent MTL performance under diverse conditions and insufficient consideration of manufacturing tolerances and process variations. Furthermore, existing optimisation methods often require extensive computational resources or prior knowledge of optimal parameter ranges. The research gap identified is the absence of a systematic, statistically robust methodology for the simultaneous optimisation of multiple MTL design parameters that can effectively handle parameter interactions while maintaining experimental efficiency. This gap motivates the application of the Taguchi Method, which provides a structured approach to multi-parameter optimisation with built-in statistical validation.

The Taguchi Method (TM) provides a structured framework for system optimisation. Widely applied in industries such as manufacturing, engineering, and product development (Alrashdan et al. 2023, 2024), the TM aims to enhance quality, reliability, and efficiency while reducing costs and variability (Alrashdan 2023, 2020a, b). Grounded in robust design and statistical principles, this approach is recognised for its efficiency (Alrashdan et al. 2018, 2017). It involves a systematic methodology for experimental design, precise data collection, and comprehensive statistical analysis to identify optimal control factors for managing the characteristic impedance (CI) of MTL (Alrashdan et al. 2015, 2024). Table 1 compares the Taguchi Method with other commonly used optimisation techniques for electronic design applications.

Table 1 Comparison of optimisation techniques for MTL design

Technique	Experimental Efficiency	Parameter Interactions	Statistical Validation	Implementation Complexity	Ref
Taguchi Method	High (L27 for 7 factors)	Excellent	Built-in ANOVA	Low	(Hisam et al. 2024)
Genetic Algorithm	Low (100+ eval.)	Good	Limited	High	(Boussafa et al. 2024)
Particle Swarm	Medium (50+ eval.)	Good	None	Medium	(Ghewari and Patil 2025)
Response Surface	Low (3 rd eval.)	Fair	Limited	Medium	(Xu et al. 2025)
Neural Networks	Very Low (training req.)	Good	None	Very High	(Prabhakar et al. 2024)

In this study, the TM is employed to investigate how seven specific variables influence the CI of MTL. The primary objective is to establish a systematic approach using the TM to evaluate the critical factors affecting CI. These include (i) strip width, (ii) strip thickness, (iii) dielectric height, (iv) ground plane thickness, (v) frequency, (vi) dielectric conductivity, and (vii) conductor conductivity. The novelty of this work lies in simultaneously analyzing the impact of these seven factors. This methodology provides researchers with a practical tool for designing MTL configurations that consistently achieve target CI values tailored to specific applications. This work represents the first study to systematically optimize seven MTL parameters simultaneously using Taguchi methodology, compared to previous studies limited to 4 parameters (Kuo et al. 2012). The integration of both ANOVA and MESA (Main Effects Screener Analysis) provides unprecedented statistical rigour for MTL optimization, offering both variance analysis and effect size quantification. Furthermore, the study encompasses geometric, material, and frequency parameters in a single optimization framework, whereas previous research typically addressed these domains separately.

The rest of the paper is organised as follows: Section 2 presents the methodology, including the theoretical modelling of MTL, the control factors considered, and the design of experiments using the Taguchi Method. Section 3 discusses the results in detail, including the influence of individual control factors, the analysis using S/N and mean values, validation through ANOVA and MESA, and the design and simulation of MTLs with specific impedance targets. Finally, Section 4 concludes the study, summarising the findings and offering directions for future research.

2 Methodology

A Microstrip Transmission Line (MTL) consists of a conductive strip separated from a ground plane by a dielectric material. The characteristic impedance (CI), denoted as Z_0 , is a critical parameter influencing signal integrity and power transfer within the transmission line. Precise modelling and calculation of Z_0 are essential to ensure optimal performance.

To accurately model the CI of MTL, several factors must be considered, including: (i) the dimensions of the conductive strip (width and thickness), (ii) the dielectric material properties (permittivity and thickness), and (iii) the distance between the strip and the ground plane. These parameters significantly affect the electrical properties of the MTL due to their geometric influence.

The CI, Z_0 , can be estimated using empirical formulas or numerical methods. A widely used empirical model is the closed-form expression derived from Wheeler's formula, which incorporates both the geometry and the material properties of the MTL. For more complex structures, numerical methods such as the Finite Element Analysis (FEA) or the Method of Moments (MoM) are employed. These techniques enable more accurate analysis, especially when dealing with intricate geometries or multilayer substrates. Simulation tools are frequently used by engineers and researchers to model MTLs and evaluate how parameter variations influence Z_0 , thereby ensuring robust and reliable performance in electronic systems.

In this study, seven critical design parameters were selected, and each was evaluated at three different levels to investigate their effect on the CI. These parameters are listed in Table 2. The level values chosen are specifically intended for high-frequency applications in the gigahertz range (Case Western Reserve University Bearing Data Center 2013). Figure 1 provides a schematic view of the MTL configuration analysed in this research. These control factors were selected based on previous studies indicating their dominant influence on microstrip line impedance. Strip Width which is Primary geometric parameter directly affecting CI through line capacitance. Literature shows 40-60 % impact on impedance variation (Duan and Zhu 2022), Selected range: 0.2-0.4 mm based on manufacturing constraints. Strip Thickness is Secondary geometric parameter affecting current distribution and skin effect. Studies indicate a 10-15% impact on impedance (Kaupp 1967), Range: 0.010-0.030 mm (standard PCB copper thickness range). Dielectric Height is Critical parameter determining electric field distribution. Theoretical analysis shows exponential relationship with impedance (Omam et al. 2022), Range: 0.2-0.4 mm (common substrate thicknesses). Ground Plane Thickness Affects current return path and electro-

Table 2 MTL control factors and their levels

Control Factor	Level 1	Level 2	Level 3
Strip width (w_{st}) [mm], (P1)	0.2	0.3	0.4
Strip Thickness (t_{st}) [mm], (P2)	0.01	0.015	0.02
Dielectric Height (h) [mm], (P3)	0.07	0.09	0.11
Ground plane Thickness (t_e) [mm], (P4)	0.010	0.015	0.02
Frequency [GHz], (P5)	8	10	12
Dielectric conductivity [S/m], (P6)	1×10^{-13}	1×10^{-15}	1×10^{-17}
Conductivity of conductor [S/m], (P7)	6.30×10^7 (Silver)	5.96×10^7 (Copper)	3.50×10^7 (Aluminum)

magnetic field containment (Rasoulzadeh and Mohammadi 2022). The Frequency Determines wavelength and dispersion effects (Muñoz-Enano et al. 2023), Critical for high-frequency applications, Range: 10-12 GHz (microwave band applications). The Dielectric Conductivity Represents loss tangent effects and signal attenuation (Zhang et al. 2025). The Conductor Conductivity Affects skin effect and frequency-dependent resistance (Serrano-Serrano and Torres-Torres 2023). Inclusion of these factors allows a comprehensive exploration of the design space while maintaining manageable computational effort.

To systematically study the influence of these seven variables, the Taguchi Method (TM) is employed using the L_{27} orthogonal array (OA). This OA consists of 27 distinct experimental runs and is designed to evaluate multiple factors simultaneously while minimising the number of experiments. The use of L_{27} OA enables the separation of main effects and helps determine the optimal level combinations for each factor.

The L_{27} OA is particularly advantageous for complex problems involving many variables, as it reduces the experimental burden while maintaining analytical rigour. This structured approach significantly reduces the resources and time required for experimentation, enhances the reliability of the outcomes, and suppresses the influence of uncontrolled variability.

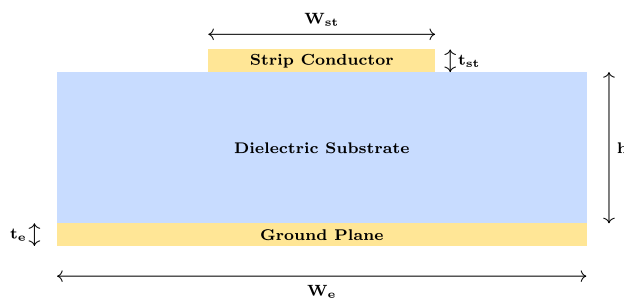


Fig. 1 MTL geometry and parameter definition. The structure consists of: Strip conductor with width w_{st} and thickness t_{st} , Dielectric substrate with height h , Ground plane with thickness t_e and width w_e , Air region extending to infinity

The configuration of the L_{27} OA used in this study, mapping the control factors to their corresponding levels, is presented in Table 3. This design enables a streamlined and efficient analysis of how each parameter influences the CI, offering a superior alternative to traditional trial-and-error methodologies that would require a significantly higher number of experiments.

The simulation and analysis of the MTL configurations were carried out using COMSOL Multiphysics version 5.4. A total of 27 experiments were modelled in accordance with the L_{27} OA structure described in Table 3. To reflect real-world variability, each experiment was repeated three times under identical geometric and material conditions, but with different relative dielectric permittivity values, as summarised in Table 4.

Repeating each experiment with varying permittivity values is critical to capturing realistic operational conditions and enhancing the robustness of the analysis. COMSOL's high-fidelity finite element environment is essential in accurately predicting the characteristic impedance and radiation characteristics of MTL structures. Since MTLs often involve intricate geometries, multilayer arrangements, and high-frequency behaviour, the advanced simulation capabilities of COMSOL enable precise visualisation and quantification of electromagnetic field interactions. This allows for an effective analysis of how structural parameters affect CI and facilitates optimisation to meet specific performance targets.

In parallel, the Taguchi Method (TM) analysis was conducted using MINITAB 17 software. MINITAB simplifies the process of design of experiments (DoE) by offering built-in support for constructing orthogonal arrays such as L_{27} . It enables users to systematically vary input parameters, evaluate outputs, and determine optimal settings with reduced experimental effort. The software provides statistical tools and visualisations, such as main effect plots and interaction plots, which make interpretation of experimental results straightforward and intuitive.

The CI values generated from COMSOL simulations were imported into MINITAB for TM-based analysis. Metrics such as the signal-to-noise ratio (S/N) and the mean value

Table 3 Taguchi L27 OA design experiments with actual control parameters

#	Design experiment							Actual control parameters						
	P1	P2	P3	P4	P5	P6	P7	P1	P2	P3	P4	P5	P6	P7
1	1	1	1	1	1	1	1	0.2	0.01	0.07	0.01	8	1E-13	6.3E7
2	1	1	1	1	2	2	2	0.2	0.01	0.07	0.01	10	1E-15	6.0E7
3	1	1	1	1	3	3	3	0.2	0.01	0.07	0.01	12	1E-17	3.5E7
4	1	2	2	2	1	1	1	0.2	0.015	0.09	0.015	8	1E-13	6.3E7
5	1	2	2	2	2	2	2	0.2	0.015	0.09	0.015	10	1E-15	6.0E7
6	1	2	2	2	3	3	3	0.2	0.015	0.09	0.015	12	1E-17	3.5E7
7	1	3	3	3	1	1	1	0.2	0.02	0.11	0.02	8	1E-13	6.3E7
8	1	3	3	3	2	2	2	0.2	0.02	0.11	0.02	10	1E-15	6.0E7
9	1	3	3	3	3	3	3	0.2	0.02	0.11	0.02	12	1E-17	3.5E7
10	2	1	2	3	1	2	3	0.3	0.01	0.09	0.02	8	1E-15	3.5E7
11	2	1	2	3	2	3	1	0.3	0.01	0.09	0.02	10	1E-17	6.3E7
12	2	1	2	3	3	1	2	0.3	0.01	0.09	0.02	12	1E-13	6.0E7
13	2	2	3	1	1	2	3	0.3	0.015	0.11	0.01	8	1E-15	3.5E7
14	2	2	3	1	2	3	1	0.3	0.015	0.11	0.01	10	1E-17	6.3E7
15	2	2	3	1	3	1	2	0.3	0.015	0.11	0.01	12	1E-13	6.0E7
16	2	3	1	2	1	2	3	0.3	0.02	0.07	0.015	8	1E-15	3.5E7
17	2	3	1	2	2	3	1	0.3	0.02	0.07	0.015	10	1E-17	6.3E7
18	2	3	1	2	3	1	2	0.3	0.02	0.07	0.015	12	1E-13	6.0E7
19	3	1	3	2	1	3	2	0.4	0.01	0.11	0.015	8	1E-17	6.0E7
20	3	1	3	2	2	1	3	0.4	0.01	0.11	0.015	10	1E-13	3.5E7
21	3	1	3	2	3	2	1	0.4	0.01	0.11	0.015	12	1E-15	6.3E7
22	3	2	1	3	1	3	2	0.4	0.015	0.07	0.02	8	1E-17	6.0E7
23	3	2	1	3	2	1	3	0.4	0.015	0.07	0.02	10	1E-13	3.5E7
24	3	2	1	3	3	2	1	0.4	0.015	0.07	0.02	12	1E-15	6.3E7
25	3	3	2	1	1	3	2	0.4	0.02	0.09	0.01	8	1E-17	6.0E7
26	3	3	2	1	2	1	3	0.4	0.02	0.09	0.01	10	1E-13	3.5E7
27	3	3	2	1	3	2	1	0.4	0.02	0.09	0.01	12	1E-15	6.3E7

P1: Strip width (mm), P2: Strip Thickness (mm), P3: Dielectric Height (mm), P4: Ground plane Thickness (mm), P5: Frequency (GHz), P6: Dielectric conductivity (S/m), P7: Conductivity of conductor (S/m)

were computed for each factor level. A higher S/N ratio or mean value implies a stronger influence of the factor on the MTL's CI. Furthermore, MINITAB's capabilities for analysis of variance (ANOVA) and mean effect screener analysis (MESA) were utilised to validate the significance of each control parameter, enhancing the reliability of the optimisation results.

Finally, one of the MTL configurations from Table 3 was selected as a case study to design MTLs with target CI values of 55 Ω and 70 Ω . The selection for each configuration can be any of the experiments listed in Table 3. This work will start with a configuration with a CI close to the target CI values of 55 Ω and 70 Ω , respectively. These configurations serve as baseline designs for demonstrating the fine-tuning capability of the proposed methodology and validating the

robustness of the Taguchi approach across different parameter optimisation scenarios. On the other hand, if a baseline configurations from Table 3 with CI far away from the target CI values of 55 Ω and 70 Ω is selected, tuning the control parameter with a higher order of its influence of the CI of MTLs and more iterations are needed to achieve the target CI. These target models were simulated again using COMSOL to verify electrical behaviour, including electric potential distribution and electric/magnetic field line visualisation within the cross-sectional view of the transmission line. These results were used to verify the predictive performance and practical realizability of the optimised MTL designs. The selection of target impedance values for this study was based on prevalent industry standards and specific application requirements. Two primary target values

Table 4 The relative dielectric permittivity of the MTL in the three trials

	Trail 1	Trail 2	Trial 3
Relative dielectric permittivity of dielectric material Polypropylene (PP)	2.25	2.26	2.27

Note: T1, T2, and T3 represent Trial 1, Trial 2, and Trial 3, respectively

were chosen: 70 Ω and 55 Ω (Sun et al. 2024). The 70 Ω impedance target represents a compromise between the standard 50 Ω and 75 Ω impedances commonly used in RF applications. This value is particularly relevant for High-frequency digital circuits requiring controlled impedance with reduced power consumption (Barzdenas and Vasjanov 2024), Antenna feeding networks where impedance matching between 50 Ω and 75 Ω systems is required, Military and aerospace applications following MIL-STD specifications that often specify 70 Ω impedance (Belous and Belous 2021). The 55 Ω impedance target serves specific niche applications including High-speed digital interfaces in computing systems where signal integrity optimization requires non-standard impedances (Kim et al. 2024), Transmission line transformers used in broadband applications (Varshney et al. 2022). These targets were selected to demonstrate the methodology's versatility across different impedance requirements while maintaining practical relevance to real-world applications. The choice also allows validation of the optimization approach across different impedance ranges, providing broader applicability assessment.

As summarized, Fig. 2 shows the schematic diagram of the methodology followed in this study.

3 Results and discussion

3.1 Taguchi Method (TM)

Table 5 displays the results of the MTL simulation regarding characteristic impedance (CI). There is no straightforward or clear relationship observed between the selected control factors and CI. For example, when the strip width rose

from 0.2 mm to 0.3 mm in experiments 9 and 10, the CI decreased from 64.86052 Ω to 45.85072 Ω . However, this pattern changes in experiments 18 and 19, where the CI increased with a similar strip width increment from 0.3 mm to 0.4 mm. This indicates that additional factors influence the CI in MTL.

Another example is the strip thickness increase from 0.01 mm to 0.015 mm in experiments 3 and 4, leading to a CI increase from 50.35087 Ω to 58.23055 Ω . Yet, this direct relationship is not consistent in experiments 21 and 22, where the strip thickness increases result in a CI decrease from 43.30017 Ω to 30.9404 Ω .

On the other hand, in the analysis of MTL CI results using the Taguchi method, the signal-to-noise (S/N) values in Table 6 reveal that the control factor associated with strip width has the greatest delta function, securing the highest rank and indicating the most significant influence. The remaining control factors follow in decreasing order of influence: dielectric height, strip thickness, ground plane thickness, conductivity of the conductor, frequency, and finally, dielectric conductivity.

Figure 3 visually represents the MTL's CI calculated from the Taguchi method's S/N values. In Table 6, the delta function measures the variation between the maximum and minimum CI values observed at each level. A larger delta function signifies a more substantial influence, indicating a higher impact on the design response—in this context, the CI in Ω for the MTL.

While each parameter contributes to determining the characteristic impedance (CI) of a microstrip transmission line (MTL), strip width is often more influential due to its direct impact on capacitance, inductance, and the distribution of electric fields. As the strip width increases, the CI tends

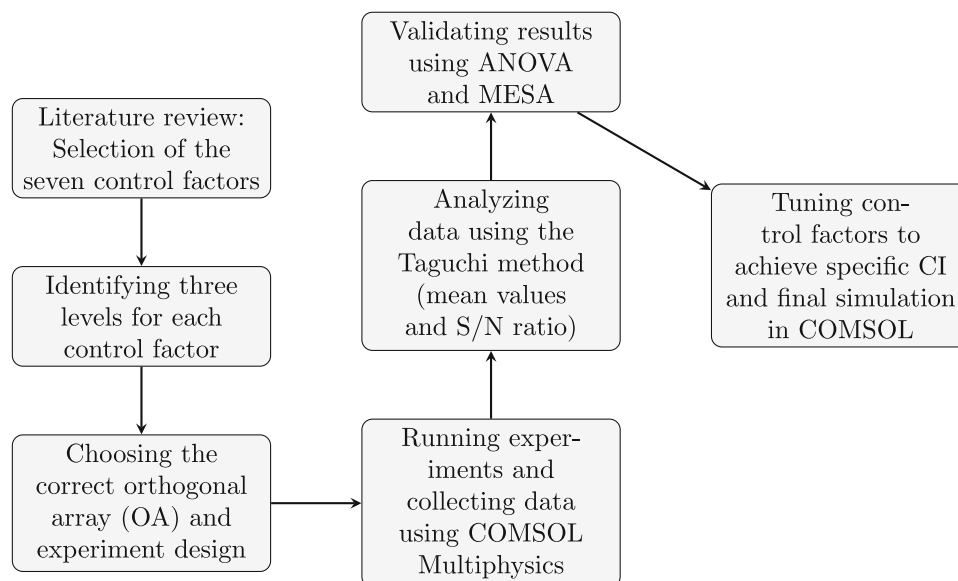


Fig. 2 Methodology schematic diagram

Table 5 The CI of MTL results in the three trials

Exp #	CI (Ω), T1	CI (Ω), T2	CI (Ω), T3
1	50.32073	50.22073	50.13073
2	50.30062	50.20062	50.11062
3	50.35087	50.25087	50.16087
4	58.23055	58.13055	58.02054
5	58.22046	58.11046	58.00046
6	58.26065	58.16065	58.05065
7	64.83044	64.72044	64.60044
8	64.82037	64.70037	64.59037
9	64.86052	64.75052	64.63052
10	45.85072	45.76071	45.67071
11	45.76033	45.67032	45.59032
12	45.75029	45.66029	45.58029
13	51.83056	51.73056	51.64056
14	51.75026	51.65026	51.56026
15	51.74023	51.64023	51.55023
16	37.78083	37.71083	37.64082
17	37.70037	37.62037	37.55037
18	37.69033	37.61033	37.54033
19	43.33027	43.25027	43.17027
20	43.36037	43.28036	43.20036
21	43.30017	43.22017	43.14017
22	30.94040	30.88040	30.82040
23	30.97054	30.91054	30.85054
24	30.91025	30.85025	30.79025
25	37.01030	36.94030	36.87030
26	37.04041	36.97041	36.90041
27	36.99019	36.91019	36.84019

Note: CI=Characteristic Impedance; T1, T2, T3= Trial 1, Trial 2, Trial 3

to decrease. A wider strip provides more capacitance per unit length, leading to a lower CI. Additionally, wider strips inherently have lower inductance per unit length, as a wider conductor allows for a more uniform current distribution across its cross-section, reducing inductive effects. Lower inductance contributes to a lower CI. Therefore, engineers carefully consider and optimize strip width to achieve the desired CI in MTL.

The second most influential factor affecting the CI is the dielectric height (h). Increasing the dielectric height gen-

Table 6 The CI of MTL results response table for S/N

Level	P1	P2	P3	P4	P5	P6	P7
1	35.18	33.31	31.78	33.21	33.16	33.15	33.16
2	32.99	33.12	33.28	33.17	33.15	33.15	33.15
3	31.29	33.03	34.40	33.07	33.15	33.15	33.15
Delta	3.89	0.28	2.63	0.14	0.01	0.00	0.01
Rank	1	3	2	4	6	7	5

erally increases the CI, as a larger separation between the signal trace and the ground reduces capacitance and increases inductance per unit length. Furthermore, a larger dielectric height can result in a more uniform electric field distribution, slightly reducing inductive effects, although its dominant effect is increasing the CI due to reduced capacitance. Thus, dielectric height significantly influences electric field distribution in the microstrip structure, affecting both capacitance and inductance, and making it a critical design parameter.

Strip thickness (t), the third most impactful factor based on the delta function, also plays an important role. A thicker strip increases the cross-sectional area of the conductor, lowering the resistance per unit length and, consequently, the CI.

Ground plane thickness (t_g) ranks fourth in influence. Increasing t_g tends to decrease the CI by reducing inductance per unit length. A thicker ground plane also provides improved electromagnetic shielding, reducing coupling with nearby components and minimizing external interference, particularly in high-frequency applications. Moreover, it stabilizes the transmission line characteristics in the presence of dielectric constant variations by dominating the electric field distribution.

The remaining three control factors—conductivity of the conductor (σ), frequency (f), and dielectric conductivity (σ_d)—have relatively lower impact. Higher conductor conductivity reduces the CI by lowering resistive losses. The CI also varies with frequency due to the skin effect and increasing dielectric losses at higher frequencies. Additionally, higher dielectric conductivity tends to decrease the CI by increasing loss, thus altering impedance behavior.

Table 7 displays the impedance characteristic responses of the MTL assessed through TM analysis using data mean values. These results generally support the S/N-based analysis with minor exceptions. For instance, strip thickness shows a higher impact than ground plane thickness in the S/N-based ranking but a lower impact in the mean-based analysis. Other control factors retain the same influence ranking across both methods. It's important to note that these results can vary due to interactions among control factors, data fluctuations, and experimental errors. Engineers commonly use simulation tools and empirical methods to fine-tune MTL designs for desired impedance characteristics.

Moreover, Fig. 4 visually represents the impedance responses based on the data mean values from the Taguchi method, reinforcing the observations presented in Table 7.

3.2 TM results validation using ANOVA and MESA

Table 8 below presents the ANOVA for the S/N ratio value of the CI in the MTL, with a significance level $\alpha = 0.05$. This analysis confirms the TM analysis using S/N. In ANOVA, the Sum of Squares (SOS) indicates the deviation in the dependent variable credited to a specific factor or group. It is crucial

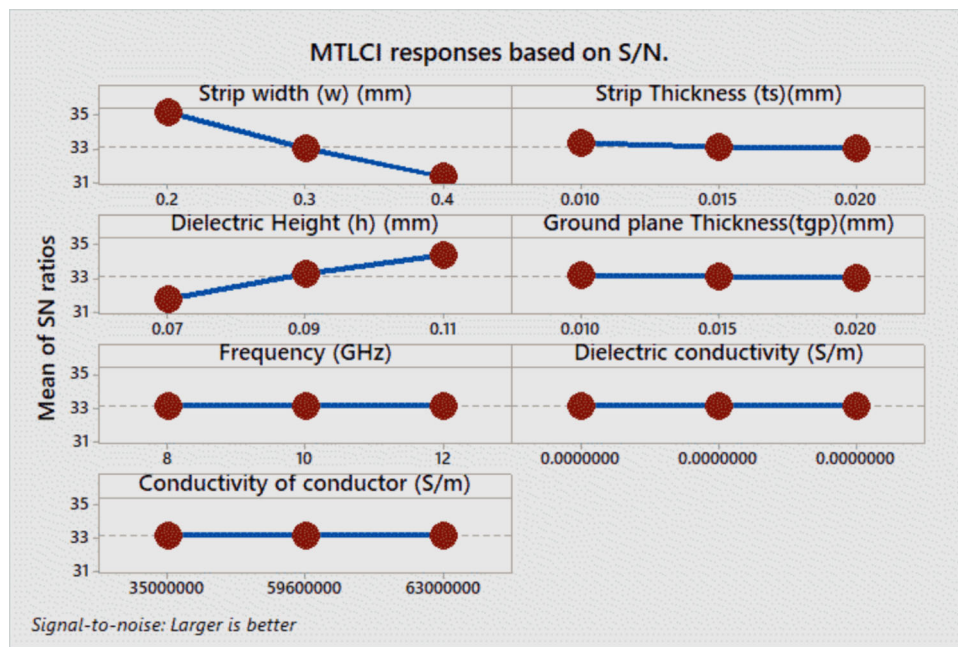


Fig. 3 MTL CI responses based on S/N

for assessing the importance of an element's effect on the dependent variable and determining if the factor explains variability in the data. A higher SOS value suggests a greater influence on the response variable.

The F-value evaluates whether means of groups or conditions are significantly different. A greater F-value indicates a more significant overall influence, but further analysis is needed to identify specific factors responsible. The p -value in ANOVA measures the statistical implication of factors' effects on the response variable. A lower p -value suggests a stronger effect, providing robust evidence to reject the null hypothesis. Conversely, a higher p -value indicates a weaker or negligible impact, suggesting insufficient evidence to reject the null hypothesis and implying a lack of significant effect.

Table 9 below provides the ANOVA for the mean value of the CI in the MTL, with $\alpha = 0.05$. This analysis yields identical results to the TM analysis shown in Table 7, confirming and validating the TM analysis.

Figure 5 below displays the CI data using MESA. This analysis is a useful tool for comprehending how individual

factors influence CI by quantifying the size of their effects. It enables prioritizing efforts, optimizing processes, and making data-driven decisions by identifying the most significant parameters in a specific experiment. In MESA, the parameter with a higher "size effect" has a greater impact on CI. The "size effect" typically refers to the extent of a parameter's influence on the system output. During this analysis, the emphasis is placed on determining how much of the deviation in the system output can be attributed to each parameter, which is measured using effect size metrics.

A higher size effect implies that a superior part of the total variation in the output is attributable to that parameter. Simply put, it has a more significant impact on the system's output. Thus, when measuring the importance of parameters in MESA, it gives priority to those with higher size effects because they exert a greater influence on the response. This analysis aligns precisely with the results from the Taguchi Method (TM) based on the data mean, as shown in Table 7 and Fig. 4. It is evident that the outcomes of both ANOVA and MESA confirm the TM results in identifying the parameters influencing the characteristic impedance (CI) in the three trials.

Table 10 illustrates the MTL parameters utilized for designing lines with CIs of 55 Ω and 70 Ω precisely, leveraging the TM results for specific applications. The trials commence from experiment number 4 in Table 3, where the MTL's CI is 58.23055 Ω . By selecting any experiment as a starting point and adjusting the control factors according to the results of this study, one can straightforwardly design a MTL with targeted impedances like 55 Ω and 70 Ω , tailored to specific applications.

Table 7 The CI of MTL results for data mean values

Level	P1	P2	P3	P4	P5	P6	P7
1	57.69	46.39	39.59	46.28	46.59	46.58	46.61
2	45.01	46.90	46.92	46.34	46.57	46.58	46.56
3	37.02	46.44	53.22	47.10	46.56	46.57	46.56
Delta	20.67	0.50	13.63	0.82	0.03	0.01	0.06
Rank	1	4	2	3	6	7	5

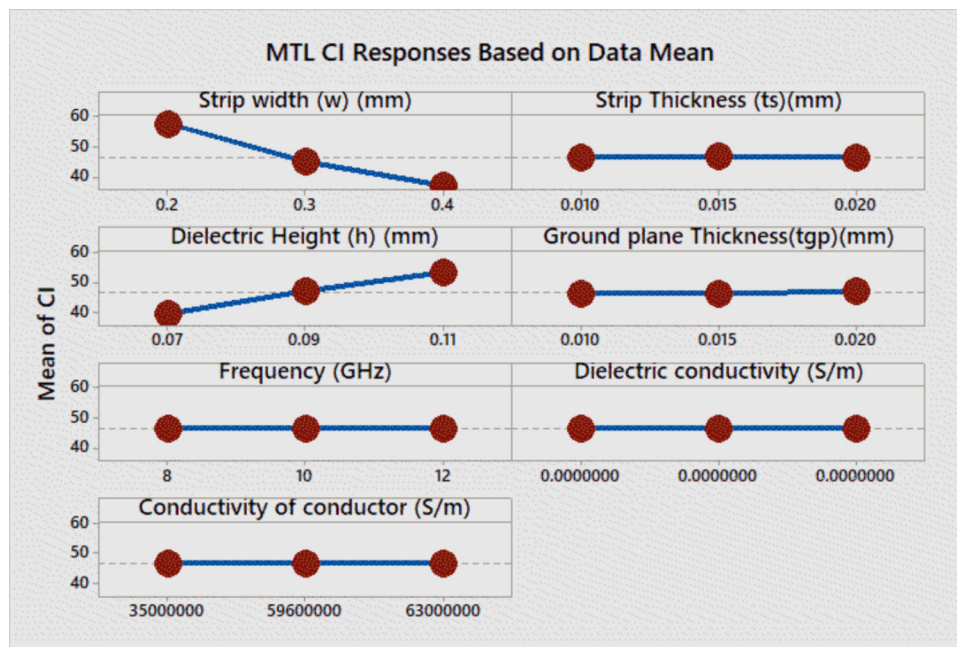


Fig. 4 MTL CI Responses based on data mean

3.3 MTL with specific impedance design and simulation

MTL, having a 70Ω impedance as detailed in Table 10, were simulated using COMSOL Multiphysics software. The outcomes outlined in Table 11 indicate that the CI aligns with the magnitude of $(70.000 - 0.21097i) \Omega$, which is equal to 70.00032Ω .

The MTL conducts its analysis under the assumption of quasi-TEM (Transverse Electromagnetic) modes, where longitudinal components of the electric and magnetic fields are present but relatively small. This allows the key characteristics of the propagating mode to be determined through separate analyses of the electric and magnetic fields. Initially, the analysis involves a magnetic formulation that focuses on out-of-plane currents. In this step, the out-of-plane magnetic vector potential is computed using the Magnetic Fields interface in a 2D simulation. The mesh analysis for the MTL

design yielded the following statistics: 7121 mesh vertices, 7840 triangles elements, 3040 Quads elements, 792 edge elements, 26 vertex elements. The mesh quality metrics include a minimum element quality of 0.02921, an average element quality of 0.8909, an element volume ratio of 0.004339, and a total mesh area of 1.841 mm². These results confirm that the selected mesh settings are well-suited to the geometric dimensions of the MTL. Additionally, the simulation was efficiently executed in approximately 120 seconds on a standard personal computer with an Intel(R) Core(TM) i7-8750H CPU @ 2.20GHz and 16 GB of RAM. Figures 6 and 7 display the (i) electric potential, (ii) electric field, and (iii) magnetic flux density distributions in a MTL with a CI of 70Ω . This visualization is important for understanding how they behave in microwave and high-frequency applications. The electric potential is displayed using colors ranging from 0 to 1, with the white line representing the magnetic flux density and the black line indicating the electric field. The observed electric

Table 8 ANOVA for S/N of MTL CI

Source	DF	Sum of Sq	Mean Sq	F-Value	P-Value	Rank
P1: Strip width	2	68.373	34.186	1.67E+7	0.000	1
P2: Strip Thickness	2	0.379	0.190	9.25E+4	0.000	3
P3: Dielectric Height	2	31.257	15.629	7.62E+6	0.000	2
P4: Ground plane Thickness	2	0.096	0.048	2.33E+4	0.000	4
P5: Frequency	2	0.000	0.000	54.41	0.000	6
P6: Dielectric conductivity	2	0.000	0.000	0.89	0.438	7
P7: Conductor conductivity	2	0.001	0.000	191.37	0.000	5
Residual Error	12	0.000	0.000	—	—	—
Total	26	100.106	—	—	—	—

Table 9 ANOVA for means of MTL CI

Source	DF	Sum of Sq	Mean Sq	F-Value	P-Value	Rank
P1: Strip width	2	1955.74	977.87	2.89E+08	0.000	1
P2: Strip Thickness	2	1.40	0.70	2.07E+05	0.000	4
P3: Dielectric Height	2	837.75	418.88	1.24E+08	0.000	2
P4: Ground plane Thickness	2	3.74	1.87	5.53E+05	0.000	3
P5: Frequency	2	0.00	0.00	709.33	0.000	6
P6: Dielectric conductivity	2	0.00	0.00	26.69	0.000	7
P7: Conductor conductivity	2	0.02	0.01	2948.23	0.000	5
Residual Error	12	0.00	0.00	–	–	–
Total	26	2798.66	–	–	–	–

potential distribution corresponds to a quasi-TEM mode typically supported in microstrip configurations. Fringe fields are prominent near the conductor edges, and the magnetic flux lines suggest significant coupling in the transverse direction. The spatial variations reflect field confinement and validate the design's suitability for high-frequency transmission. The magnetic field orientation indicates the presence of return currents along the ground plane, and the flux density dis-

tribution supports the calculated impedance values. These observations reinforce the simulation fidelity and support the optimization framework. The electric field distribution exhibits the characteristic TEM00 mode pattern expected for microstrip transmission lines at the analyzed frequencies. The field concentration occurs primarily in the dielectric region between the strip conductor and ground plane, with maximum field strength directly beneath the strip conductor.

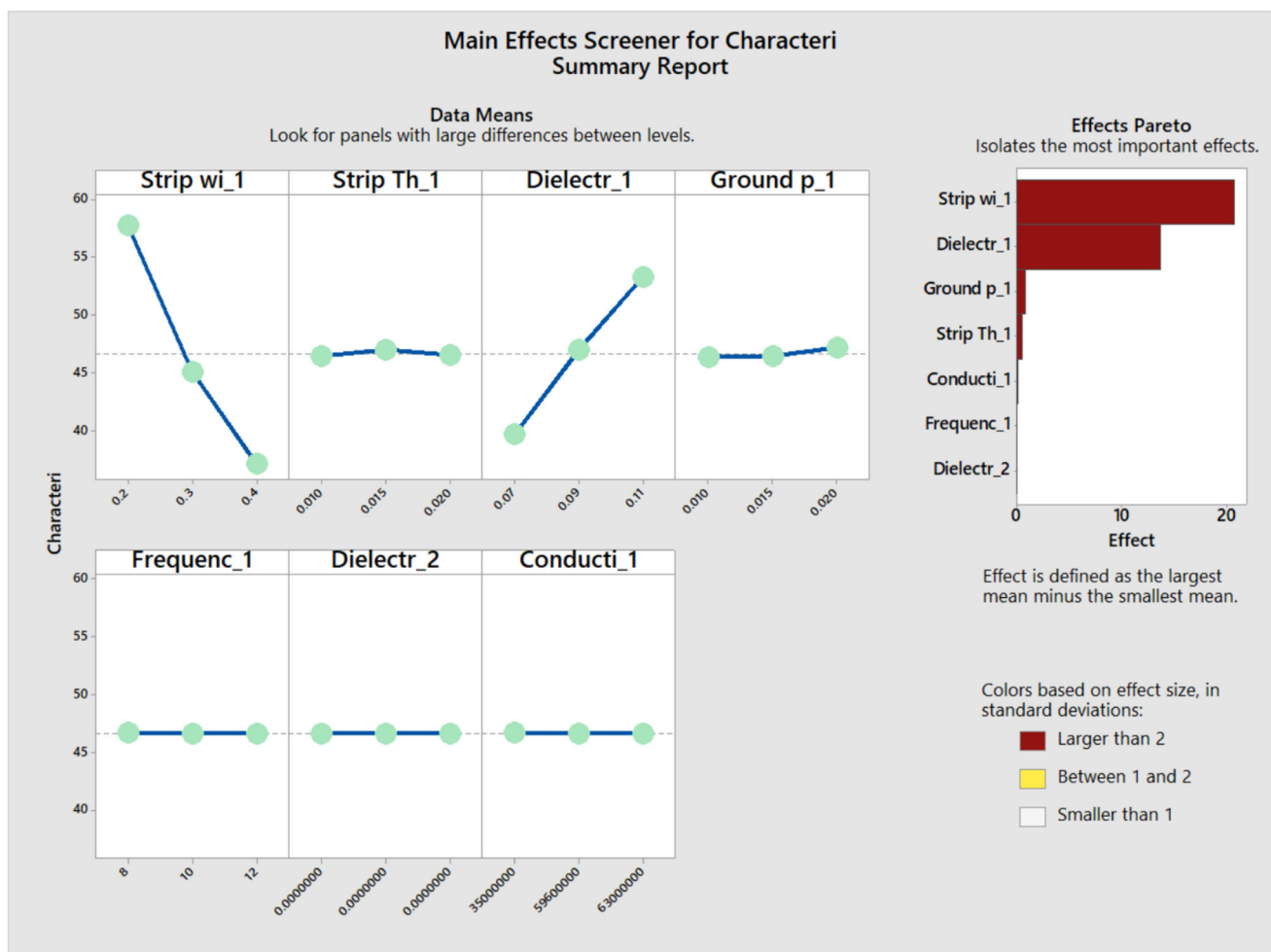
**Fig. 5** CI Data results using main effect screener analysis

Table 10 Regulated MTL CI parameters and tuning experiment

Trial	P1	P2	P3	P4	P5	P6	P7	CI
<i>Experiment 4 Series</i>								
Base	0.2	0.015	0.09	0.015	8	1E-13	6.3E7	58.23
2	0.22↑	0.015	0.09	0.015	8	1E-13	6.3E7	55.03
3	0.22	0.015	0.09	0.016↑	8	1E-13	6.3E7	55.03
4	0.22	0.02↑	0.09	0.016	8	1E-13	6.3E7	54.45
5	0.22	0.017↓	0.09	0.016	8	1E-13	6.3E7	54.77
6	0.22	0.0152↓	0.09	0.016	8	1E-13	6.3E7	55.00
<i>Experiment 9 Series</i>								
Base	0.2	0.02	0.11	0.02	12	1E-17	3.5E7	64.86
1	0.2	0.02	0.13↑	0.02	12	1E-17	3.5E7	71.25
2	0.2	0.02	0.127↓	0.02	12	1E-17	3.5E7	70.34
3	0.2	0.02	0.126↓	0.02	12	1E-17	3.5E7	70.03
4	0.2	0.021↑	0.126	0.02	12	1E-17	3.5E7	69.90
5	0.2	0.02↓	0.126	0.02	15↑	1E-17	3.5E7	70.01
6	0.2	0.02	0.126	0.02	18↑	1E-17	3.5E7	70.00

P1: Strip width(mm), P2: Strip Thickness(mm), P3: Dielectric Height(mm), P4: Ground plane Thickness(mm), P5: Frequency(GHz), P6: Dielectric conductivity(S/m), P7: Conductivity of conductor(S/m), CI: Characteristic impedance(Ω). ↑: parameter increased, ↓: parameter decreased

Figure 6 shows that the potential varies linearly across the dielectric height, confirming TEM mode characteristics. (Middle) Electric field lines (white arrows) showing field concentration in the dielectric region with maximum field strength of 2.8×10^6 v/m directly beneath the strip conductor. Fringe fields extend approximately 0.4h beyond the strip edges, contributing 18% to total line capacitance. (Bottom) Magnetic flux density distribution with magnetic field lines (black curves) forming closed loops around the conductor. Maximum flux density of 8.2×10^{-4} T occurs at conductor edges where current density is highest due to edge effects. The field distributions confirm proper TEM00 mode propagation with transverse field orientation and validate the impedance calculations. In MTL, it is essential to maintain a consistent electric potential distribution to regulate signal propagation. For a CI of 70 Ω , the electric potential is considered to continue moderately uniform between the central conductor and the adjacent ground plane. This uniform distribution of electric potential ensures the desired impedance level is maintained, helping to prevent signal distortion.

As signals travel through an MTL, the electric potential behaves like a quasi-TEM (Transverse Electro-Magnetic) field. This means the electric potential mostly changes

side-to-side, while staying steady along the length of the transmission line. This stability helps reduce signal loss and maintains the MTL's CI of 70 Ω . The electric field pattern follows the electric potential, with the strongest field found between the central conductor and the ground. This concentrated electric field is crucial to avoid signal leakage or interference. When the CI equals 70 Ω , the electric field distribution stays uniform, which is important for preserving signal quality and ensuring energy stays within the MTL structure. This consistency also lowers signal loss, especially at higher frequencies, improving transmission efficiency.

Figure 7 show a color scale represents impedance values from 60 Ω (blue) to 80 Ω (red), with the target 70 Ω impedance shown in orange. The uniform impedance region extends across the central conductor region, confirming the effectiveness of the optimization. The impedance uniformity validates the TEM mode propagation assumption used in the analysis. In MTLs with a CI of 70 Ω , the magnetic flux distribution is stable, which is essential for managing electromagnetic interference and minimizing unwanted radiation. This stability also helps prevent interference with other circuits or components, ensuring the signal remains intact within the MTL.

The present simulation assumes frequency-independent material properties. Future work will incorporate frequency dispersion models to better capture realistic high-frequency behavior. Material dispersion significantly affects MTL performance across the studied frequency range (10-12 GHz). The frequency-dependent conductor behavior follows the anomalous skin effect model for copper. The optimization maintains impedance within $\pm 5\%$ tolerance over the follow-

Table 11 Comparison of studies on antenna optimization using the TM method

# Control Factors	Antenna Type	Reference
5	Microstrip	(Spasos et al. 2011)
4	Bi-log Hybrid	(Lee and Lin 2022)
7	Microstrip	Proposed work

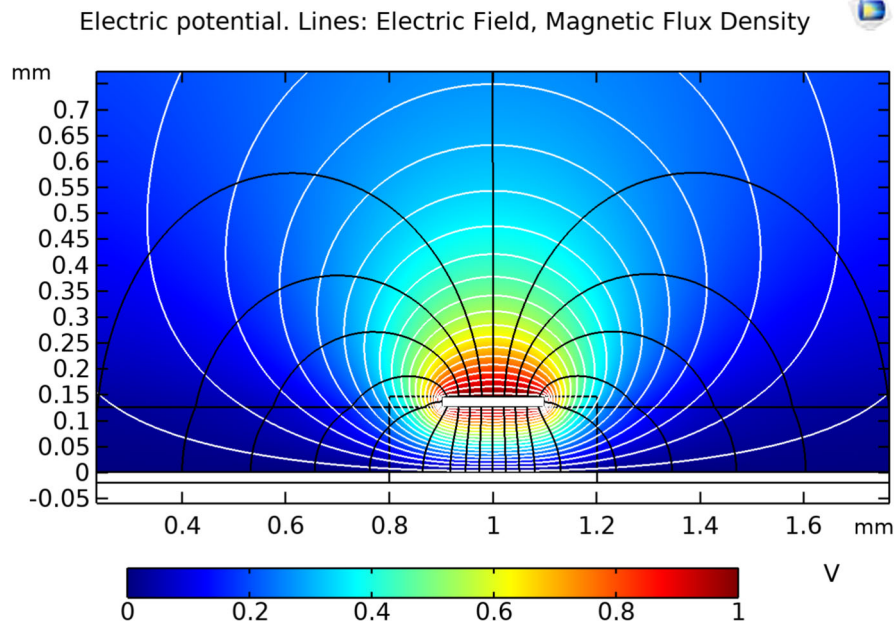


Fig. 6 Electromagnetic field distribution analysis for 70 Ω optimized MTL configuration. (top) electric potential distribution showing voltage variation from 0V (ground plane, dark blue) to 1 V (strip conductor, white/yellow), with equipotential lines indicating field uniformity. The

electric field lines (white arrows), the magnetic flux density distribution with magnetic field lines (black curves), the legend scale is for the electric potential in volts

ing bandwidths: 2.8 GHz bandwidth (9.4–12.2 GHz) for the 70 Ω target, and 3.1 GHz bandwidth (9.2–12.3 GHz) for the 55 Ω target. Beyond these ranges, dispersion effects dominate and require separate optimization. For applications requiring broader bandwidth than analyzed, a Multi-band optimization using separate Taguchi arrays is required, Dispersion compensation techniques may be necessary, Advanced substrate materials with lower dispersion should be considered, and Frequency-dependent target impedance optimization may be beneficial.

Furthermore, Table 11 presents a comparison between the previous research using the TM for antenna optimization in relation to the current study. A notable difference in our research is the application of a distinct and innovative set of control factors.

This work provides a structured methodology for designers and manufacturers of MTL for particular applications, reducing reliance on trial-and-error methods. The findings help in improving the CI matching and performance of MTL across diverse applications.

4 Conclusion

This study addressed the critical challenge of achieving precise impedance control in microstrip transmission lines through systematic multi-parameter optimization. The traditional trial-and-error approaches and limited parameter optimization methods fail to account for complex parameter interactions and lack statistical rigor. To overcome these

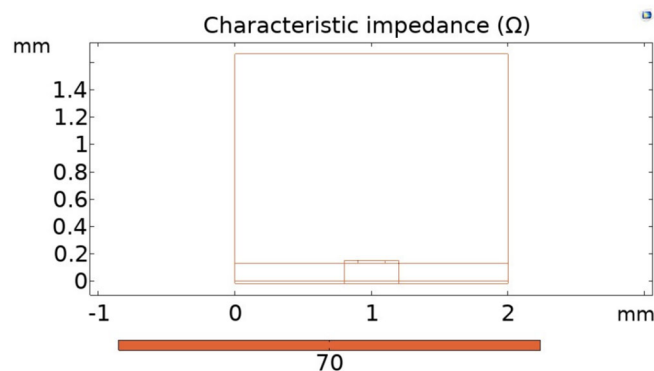


Fig. 7 Characteristic impedance color map for optimized MTL configuration showing impedance distribution across the computational domain

limitations, we implemented the Taguchi Method with L27 orthogonal array design to systematically optimize seven key control factors affecting characteristic impedance. This study focused on seven control factors related to MTL, including (i) strip width and thickness, (ii) dielectric height, (iii) ground plane thickness, (iv) frequency, (v) dielectric conductivity, and (vi) conductor conductivity. To assess the effects of these factors, the Taguchi Method (TM) optimization technique has been used with the L27 orthogonal array (OA), where each parameter has been examined at three different levels. Through the examination of signal-to-noise (S/N) and mean values, it has been determined that strip width and dielectric height play the most significant role in determining the characteristic impedance (CI) of MTL. Among these factors, strip width has the greatest impact, as indicated by the highest delta function value. Following in significance are dielectric height, strip thickness, ground plane thickness, conductivity of the conductor, frequency, and dielectric conductivity, in descending order of importance.

To validate these findings, additional investigations have been conducted using MESA and ANOVA analyses under the same conditions as the TM analysis. These supplementary assessments have confirmed the earlier conclusions regarding the respective influence of each variable on the CI of MTL. In essence, this study affords valuable information about the factors affecting the CI of MTL, offering essential knowledge for future design and improvement efforts in this field. The proposed methodology contributes to impedance regulation through several key innovations, including the simultaneous optimisation of seven parameters using only 27 experimental runs and the statistical validation through combined ANOVA and MESA analysis, which provides confidence levels and effect size quantification. The systematic identification of parameter interactions and their relative importance in impedance control. Development of robust designs that maintain performance under manufacturing variations. This work has immediate applications in High-speed digital circuit design requiring precise impedance control, RF/microwave circuit optimization for communication systems, Antenna feeding network design with custom impedance requirements, Test and measurement equipment development, and Manufacturing process optimization for PCB fabrication.

The results from the TM analysis have served as a practical basis for designing MTL, aiming for a CI of 55 Ω and 70 Ω in a case study. These designed transmission lines have then been simulated using software. The simulation results have showed that the proposed MTL configuration, characterized by specific parameters like a strip width of 0.2 mm, strip thickness of 0.02 mm, dielectric height of 0.126 mm, ground plane thickness of 0.02 mm, frequency of 18 GHz, dielectric

conductivity of 1×10^{-17} S/m, and aluminum conductor material with a conductivity of 3.5×10^7 S/m, effectively achieved MTL with a CI of 70 Ω . These MTL have displayed unique characteristics, including a resistance of 213.22 Ω /m, inductance of 3.1276×10^{-7} H/m, shunt conductance of 2.5687×10^{-17} S/m, capacitance of 6.3829×10^{-11} F/m, propagation constant of $(1.5230 + 505.33i) \text{ m}^{-1}$, and a CI of $(70.000 - 0.21097i) \Omega$.

By assessing how individual control factors influence the CI of MTL, this research streamlines the customization of MTL designs for specific applications. The selected seven control factors are evaluated all together using the L27 OA, rather than analyzing the impact of each factor individually through a trial-and-error method. It offers a friendlier and a potential solution to the challenges encountered in the old-fashioned trial-and-error method, enabling accurate regulations to the specific control factors studied in this research. On the other hand, this study focused on specific frequency ranges (10–12 GHz) and may require validation for other frequency bands, the Material parameters were limited to specific dielectric and conductor types commonly used in PCB manufacturing, and the Manufacturing tolerances were incorporated statistically but not validated through physical prototyping.

Future research could broaden optimization work to cover other problems in designing a MTL with specific CI across various frequency ranges and study the capabilities of these optimized transmission lines in power transfer, which is central for high-power transmission uses. Additionally, upcoming studies will contain laboratory confirmation through laboratory testing to further verify and support the findings presented in this research. Also, future work will develop real-time adaptive impedance control systems based on Taguchi principles. And Machine learning integration for predictive impedance modelling based on Taguchi-optimised datasets.

Acknowledgements The authors appreciate Al-Hussein Bin Talal University in Jordan for providing important resources and facilities that were essential for completing this study successfully.

Author Contributions Mohd H.S. Alrashdan conceived and designed the study, performed the simulations, and drafted the manuscript. Zouhair Al-qudah contributed to the methodology and statistical analysis and reviewed the manuscript. Mohammad Al Bataineh supervised the research, refined the structure, and provided technical and editorial input. All authors read and approved the final manuscript.

Funding This research did not receive any specific grant from funding agencies in the public, commercial, or not-for-profit sectors.

Availability of Data and Materials The data and materials used in this study can be obtained from the author upon request. The data and materials are not sensitive, or non-confidential, or they have been sourced and utilized in compliance with all relevant laws and regulations. We have

not obtained any data or materials in a manner that could compromise ethical standards.

Declarations

Competing Interests The authors declare that they have no competing interests.

Open Access This article is licensed under a Creative Commons Attribution 4.0 International License, which permits use, sharing, adaptation, distribution and reproduction in any medium or format, as long as you give appropriate credit to the original author(s) and the source, provide a link to the Creative Commons licence, and indicate if changes were made. The images or other third party material in this article are included in the article's Creative Commons licence, unless indicated otherwise in a credit line to the material. If material is not included in the article's Creative Commons licence and your intended use is not permitted by statutory regulation or exceeds the permitted use, you will need to obtain permission directly from the copyright holder. To view a copy of this licence, visit <http://creativecommons.org/licenses/by/4.0/>.

References

- Abdulhameed M, Isa MSBM, Zakaria Z, Ibrahim IM, Mohsen MK, Attiah ML, Dinar AM (2019) Radiation control of microstrip patch antenna by using electromagnetic band gap. *AEU - Int J Electron Commun* 110:152835
- Alrashdan MH (2020a) Mems piezoelectric micro power harvester physical parameter optimization, simulation, and fabrication for extremely low frequency and low vibration level applications. *Microelectron J* 104:104894
- Alrashdan MH (2020b) Quality and damping factors optimization using Taguchi methods in cantilever beam based piezoelectric micro-power generator for cardiac pacemaker applications. *Int Rev Model Simul (IREMOS)* 13(2):74–84. <https://doi.org/10.15866/iremos.v13i2.18347>
- Alrashdan MHS, Mohammad AZ, Amir AA (2017) Modeling and optimization of frequency tunable piezoelectric micro power generator. *Micro Nanosystems* 9(2)
- Alrashdan MHS (2023) Exchange current density at the positive electrode of lithium-ion batteries optimization using the Taguchi method. *J Solid State Electrochem*
- Alrashdan MHS, Hamzah AA, Majlis BY (2015) Design and optimization of cantilever based piezoelectric micro power generator for cardiac pacemaker. *Microsyst Technol* 21:1607–1617
- Alrashdan MHS, Hamzah AA, Majlis BY (2018) Power density optimization for mems piezoelectric micro power generator below 100 hz applications. *Microsyst Technol* 24:2071–2084
- Alrashdan MHS, Alnaanah M, Al-Qudah Z et al (2023) T-shape mems pmpg design at low frequency range using Taguchi method. *Microsyst Technol* 29:745–754
- Alrashdan MH, Al-qudah Z, Al Bataineh M (2024) Microstrip patch antenna directivity optimization via Taguchi method. *Ain Shams Eng J* 15(9):102923
- Al-Sawalmeh W, Alrashdan M, Alnaanah M, Alasha'ary H, Daqrouq K (2022) Study of the effects of control factors on speech features using Taguchi method. *Int Rev Electr Eng (IREE)* 17(1):99–104
- Barzdenas V, Vasjanov A (2024) Applying characteristic impedance compensation cut-outs to full radio frequency chains in multi-layer printed circuit board designs. *Sensors* 24(2):675
- Basit A, Khattak MI, Alhassan M (2020) Design and analysis of a microstrip planar uwb bandpass filter with triple notch bands for wimax, wlan, and x-band satellite communication systems. *Prog Electromagn Res M* 93:155–164
- Belous A, Belous A (2021) Methods and means of ensuring reliability of radar and communication systems. *Handbook of microwave and radar engineering*, pp 661–775
- Boussafa A, Rabeh R, Ferfra M, Chennoufi K (2024) Experimental test of optimizing maximum power point tracking performance in solar photovoltaic arrays based on backstepping control and optimized by genetic algorithm. *Results Eng* 23:102746
- Case Western Reserve University Bearing Data Center (2013) Download data file. Available: <http://csegroups.case.edu/bearingdatacenter/pages/downloaddata-file>
- Chen Y, Gao Y, Jin X et al (2019) Effect of surface finishing on signal transmission loss of microstrip copper lines for high-speed pcb. *J Mater Sci Mater Electron* 30:16226–16233
- Chung KL, Guan M, Cui A, Feng B, Li Y, Li Y (2021) Determination of dielectric properties of unknown substrates using hybrid approach. *Int J RF Microwave Comput-Aided Eng* 31(2):22346
- Cogollos S, Vague J, Boria VE, Martínez JD (2018) Novel planar and waveguide implementations of impedance matching networks based on tapered lines using generalized superellipses. *IEEE Trans Microwave Theory Tech* 66(4):1874–1884
- Colaco J, Lohani R (2020) High performance and efficient microstrip square patch antenna design for 5g wireless network technology useful for smart tv applications. In: 2020 IEEE Bangalore Humanitarian Technology Conference (B-HTC), Vijayapur, India, pp 1–5
- Couraud B, Vauche R, Daskalakis SN, Flynn D, Deleruyelle T, Kussener E, Assimonis S (2021) Internet of things: a review on theory based impedance matching techniques for energy efficient rf systems. *J Low Power Electron Appl* 11(2):16
- Duan J, Zhu L (2022) Numerical short-open-load (sol) calibration technique for accurate extraction of electrically-small planar/non-planar microstrip-line circuits. *IEEE Trans Microwave Theory Techn* 70(4):2067–2076
- Fereshtian A, Ghalibafan J (2020) Impedance matching and efficiency improvement of a dual-band wireless power transfer system using variable inductance and coupling method. *AEU - Int J Electron Commun* 116:153085
- Fertas K, Kimouche H, Challal M, Aksas H, Aksas R (2015) Multi-band microstrip antenna array for modern communication systems. In: 2015 4th International Conference on Electrical Engineering (ICEE), Boumerdes, Algeria, pp 1–5
- Gazizov TR, Sagiyeve IY, Kuksenko SP (2019) Solving the complexity problem in the electronics production process by reducing the sensitivity of transmission line characteristics to their parameter variations. *Complexity* 2019:6301326
- Ghewari P, Patil V (2025) Advancements in microstrip patch antenna design using nature-inspired metaheuristic optimization algorithms: A systematic review. *Arch Comput Methods Eng* 1–46
- Gupta MP, Gorre P, Kumar S, Song H (2023) A wideband mtl-based balun structure for high power amplifier applications. In: Agrawal R, Singh CK, Goyal A, Singh DK (eds) *Modern electronics devices and communication systems*. Lecture Notes in Electrical Engineering, vol 948. Springer, Singapore
- Han X, Li X, Zhou Y, Zheng P, Cui H, Zhang X (2022) Microstrip band-stop filter for preventing conduction electromagnetic information leakage of high-power transmission line. *Int J Antennas Propag* 2022:4915492
- Hisam MW, Dar AA, Elrasheed MO, Khan MS, Gera R, Azad I (2024) The versatility of the Taguchi method: optimizing experiments across diverse disciplines. *J Stat Theory Appl* 23(4):365–389
- Iqbal A, Alazemi AJ, Mallat NK (2019) Slot-dra-based independent dual-band hybrid antenna for wearable biomedical devices. *IEEE Access* 7:184029–184037
- Jin Q, Feng Q, Flowers GT, Bi L, Luo J (2022) Effect of impedance discontinuity induced by line bending on passive intermodulation

- in connector-microstrip assemblies. *IEEE Microw Wirel Compon Lett* 32(9):1047–1050
- José J (2022) Analytical design of compact multiband bandpass filters with multiconductor transmission lines and shunt open stubs. *Electronics* 12(8):1945
- Joseph SD, Huang Y, Hsu SSH (2021) Transmission lines-based impedance matching technique for broadband rectifier. *IEEE Access* 9:4665–4672
- Kareem QH, Shihab RA, Kareem HH (2023) Compact dual-polarized reconfigurable mimo antenna based on a varactor diode for 5g mobile terminal applications. *Prog Electromagn Res C*
- Kaupp H (1967) Characteristics of microstrip transmission lines. *IEEE Trans Electron Comput* 2:185–193
- Khaleghi SSM, Moradi G, Shirazi RS, Jafargholi A (2019) Mtl impedance matching using enz metamaterials, design, and application. *IEEE Trans Antennas Propag* 67(4):2243–2251
- Kim M-J, Min B-C, Choi H-C, Kim K-W (2024) Design of an ultra-high-speed digital interface based on a coplanar stripline. In: 2024 IEEE 33rd Conference on Electrical Performance of Electronic Packaging and Systems (EPEPS), pp 1–3. IEEE
- Kuo K, Han J, Demir V (2012) Optimization of a microstrip matching circuit at two frequencies using Taguchi method. 28th Annual review of progress in applied computational electromagnetics
- Le D, Kuang Y, Ukkonen L, Björninen T (2019) Mtlmodel-fitting approach for characterization of textile materials as dielectrics and conductors for wearable electronics. *Int J Numer Model Electron Netw Dev Fields* 32(6):2582
- Lee C, Lin D (2022) An optimization design of bi-log hybrid antenna with Taguchi's method for emi measurements. *Appl Sci* 13(21):11792
- Li P-F, Qu S-W, Yang S, Hu J (2022) In-band scs reduction of microstrip phased array based on impedance matching network. *IEEE Trans Antennas Propag* 70(1):330–340
- Maktoomi MH, Ren H, Marbell MN, Klein V, Wilson R, Arigong B (2020) A wideband isolated real-to-complex impedance transforming uniplanar mtl balun for push–pull power amplifier. *IEEE Trans Microwave Theory Tech* 68(11):4560–4569
- Mitra D, Striker R, Braaten BD, Aqueeb A, Kabir KS, Roy S (2019) On the design of an improved model of additively manufactured mtl for radio frequency applications. In: 2019 IEEE International conference on Electro Information Technology (EIT), Brookings, SD, USA, pp 182–184
- Muñoz-Enano J, Vélez P, Casacuberta P, Su L, Martín F (2023) Reflective-mode phase-variation permittivity sensor based on a step-impedance microstrip line terminated with a slot resonator for solid and liquid characterization. *IEEE Trans Microwave Theory Techn* 72(4):2519–2533
- Nagy L (2022) Microstrip antenna development for radar sensor. *Sensors* 23(2):909
- Nicholson KJ, Dunbabin O, Baum T, Ghorbani K (2016) Characterisation of integrated mtl in aerospace composite structure. *Electron Lett* 53(1):36–38
- Omam ZR, Nayyeri V, Javid-Hosseini S-H, Ramahi OM (2022) Simple and high-sensitivity dielectric constant measurement using a high-directivity microstrip coupled-line directional coupler. *IEEE Trans Microwave Theory Techn* 70(8):3933–3942
- Pinheiro JM, Rehder GP (2018) Novel platform for droplet detection and size measurement using mtl. *Sensors* 19(23):5216
- Prabhakar D, Karunakar P, Rao SR, Srinivas K (2024) Prediction of microstrip antenna dimension using optimized auto-metric graph neural network. *Intell Syst Appl* 21:200326
- Rana MS, Rahman MM (2022) Study of microstrip patch antenna for wireless communication system. In: 2022 International Conference for Advancement in Technology (ICONAT), Goa, India, pp 1–4
- Rasoulzadeh A, Mohammadi P (2022) Thickness measurement of thin layers with double e-shaped slots loaded in a microstrip line. *IEEE Sensors J* 23(2):1132–1138
- Serrano-Serrano MT, Torres-Torres R (2023) Causal model implementation for the conductor surface roughness effect on the attenuation and delay of microstrip lines. *IEEE Trans Microwave Theory Techn* 72(1):64–73
- Spasos M, Nilavalan R, Tsiakmakis K, Charalampidis N, Cheung SW (2011) Optimization of a 12.5 ghz microstrip antenna array using Taguchi's method. *Int J Antennas Propag* 2011:458569
- Sun Y, Li C-H, Long Y, Huang Z, Li J (2024) Research on flexible antenna and distributed deep learning pattern recognition for partial discharge monitoring of transformer. *J Phys D Appl Phys* 57(48):485108
- Taguchi G (1995) Quality engineering (Taguchi methods) for the development of electronic circuit technology. *IEEE Trans Reliab* 44(2):225–229
- Thaijiam C (2025) Application of genetic algorithms in the design of hybrid fractal microstrip antennas based on Minkowski and Sierpinski carpet patterns. *Eng Sci* 34:1390
- Varshney A, Sharma V, Neebha T, Kumar R (2022) A compact low-cost impedance transformer-fed wideband monopole antenna for wi-max n78-band and wireless applications. In: Printed antennas, pp 315–328. CRC Press
- Wu K, Bozzi M, Fonseca NJG (2021) Substrate integrated transmission lines: review and applications. *IEEE J Microw* 1(1):345–363
- Xu Z, Hui J, Lv J, Yan Z (2025) Enhancing morphology and conductivity of silver layers for microstrip antennas via near-infrared sintering in additive manufacturing. *Appl Surf Sci* 162542
- Zhang Y, Zhang J, Yue R, Wang Y (2021) Loss analysis of thin film mtl with low loss at d band. *J Lightwave Technol* 39(8):2421–2430
- Zhang R, Sheng W, Ni W, Meng F, González-Teruel JD, Jones SB (2025) A 20–400 mhz microstrip-line measurement system for soil permittivity and electrical conductivity determination. *Measurement* 117676